Anthropomorphic Robot Hand: Gifu Hand III

Tetsuya Mouri[*], Haruhisa Kawasaki[**], Keisuke Yoshikawa[**], Jun Takai[**], and Satoshi Ito[**]

*Virtual System Laboratory, Gifu University, Yanagido 1-1, Gifu 501-1193, Japan
(Tel : 81-58-293-3143; Fax : 81-58-293-3143; E-mail: tmouri@vsl.gifu-u.ac.jp)
**Faculty of Engineering, Gifu University, Yanagido 1-1, Gifu 501-1193, Japan
(Tel : 81-58-293-2546; Fax : 81-58-293-2546; E-mail: h_kawasa@cc.gifu-u.ac.jp, satoshi@robo.mech.gifu-u.ac.jp)

Abstract: This paper presents an anthropomorphic robot hand called Gifu Hand III, which is a modified version of Gifu Hand II. The Gifu Hand is aimed to be used as a platform of robot hands for robotics research. The Gifu Hand III is improved on the points of backlash of transmission, opposability of the thumb, and mobility space of fingertips. The opposability of the thumb is evaluated by a cubature of opposable space. An explicit kinematical relation between the fourth joint and the third one is shown, where the fourth joint is engaged with the third joint by a planar four-bars linkage mechanism. The distributed tactile sensor, which has grid pattern electrodes and uses conductive ink, is mounted on the hand surface. The sensor presents 235 points expansion relatively to that of the Gifu Hand II. To reduce insensitive area, the electrodes width and pitch are expanded and narrowed, respectively. In consequence, the insensitive area is reduced to 49.1%. Experiments of grasping several objects are shown. With these improvements and experiments, the Gifu hand III has a higher potential to perform dexterous object manipulations like the human hand.

Keywords: Robot Hand, Anthropomorphic Hand, Multi-Fingers, Thumb Opposability, Tactile Sensor, Grasping Reflex, Real-Time Control, Humanoid

1. Introduction

Many multi-fingered robot hands [1]-[4] have been developed. These robot hands are driven by actuators that are located in a place remote from the robot hand frame and connected by tendon cables. The elasticity of the tendon cable causes inaccurate joint angle control, and the long wiring of tendon cables may obstruct the robot motion when the hand is attached to the tip of a robot arm. To solve these problems, robot hands in which the actuators are built into the hand [5]-[8] have been developed. However, these hands present the problem that their movement is unlike the human hand because the number of fingers and the number of joints in the fingers are insufficient. Recently, many reports on the use of tactile sensors [9]-[13] have been presented, which attempted to realize adequate object manipulation involving contact with the fingers and palm. The development of the hand, which combines 6-axes force sensor attached to the fingertip and distributed tactile sensor mounted on the hand surface, has been slight.

Our group developed the Gifu Hand I [14]-[15], and the Gifu Hand II [16]. The Gifu Hand is a 5-fingered hand driven by built-in servomotors and has 20 joints with 16 DOF. To reduce the backlash in the gear transmission, which appears after long operation, the Gifu Hand is improved. This paper presents the improved robot hand called Gifu Hand III, a new developed distributed tactile sensor with 859 detecting points, and a hand controller with a real-time operating system called ART-Linux. Experiments of grasping several objects by a grasping strategy imitating human grasping reflex are shown. These results show that Gifu hand III has higher potential to perform dexterous object manipulations like the human hand.

2. Gifu Hand III

2.1 Characteristics of Gifu Hand III

An overview of the developed anthropomorphic robot hand called Gifu hand III is shown in Fig. 1. The right and left hands are symmetrically designed and each has a thumb and four fingers. The design mechanisms of the thumb and fingers are shown in Fig. 2. The structure of the hand is shown in Fig. 3. The servomotors and joints are numbered from the palm to the fingertip. The thumb has 4 joints with 4 DOF and each of the fingers has 4 joints with 3 DOF. The movement of the first joint of the thumb and of the fingers allows adduction and abduction, and that of the second joint to the fourth joint allows anteflexion and retroflexion. The main difference between the thumb and the fingers is that the fourth joint of the fingers is actuated by the third servomotor through a planar four-bars linkage mechanism. Thus, the Gifu hand III has 20
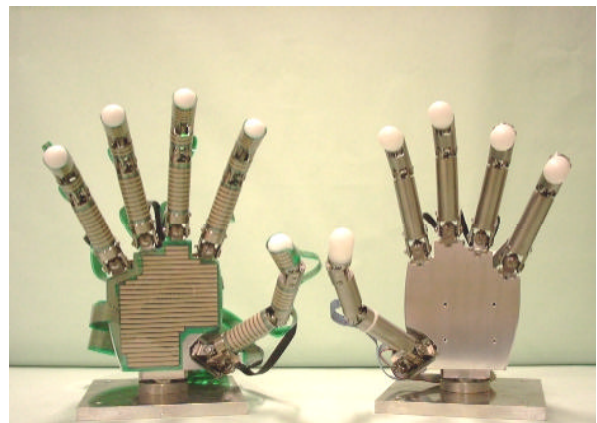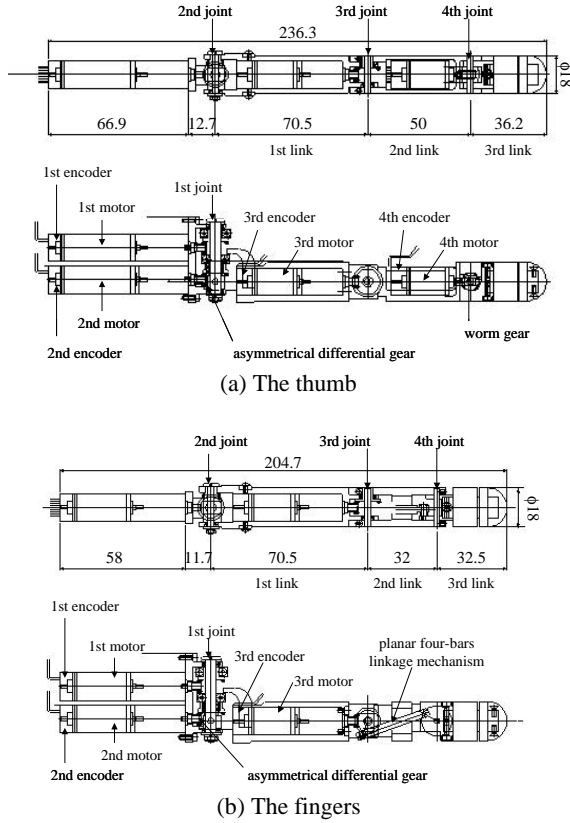

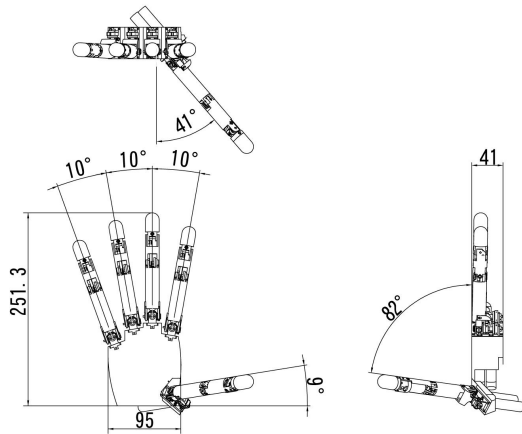Fig. 1. Developed Gifu Hand III

(a) The thumb

(b) The fingers

Fig. 2. Mechanism of the thumb and the fingers

Fig. 3. Structure of Gifu Hand III

Table 1. Specifications of the Gifu Hand III

|		
Weight	Thumb	0.25 [kgf]
	Finger	0.20 [kgf]
	Total	1.4 [kgf]
Operating angle of joints	1st joint	-28 ~ 28 [deg] (Thumb) -20 ~ 20 [deg] (Finger)
	2nd joint	-10 ~ 90 [deg]
	3rd joint	-10 ~ 90 [deg]
	4th joint	-10 ~ 90 [deg]
Output force at fingertip	Thumb	3.7 [N] [1], 2.8 [N] [2]
	Finger	3.4 [N] [1], 1.8 [N] [2]
Output torque of the thumb	1st joint	1.76 [Nm] [1], 1.03 [Nm] [2]
	2nd joint	1.27 [Nm] [1], 0.58 [Nm] [2]
	3rd joint	0.33 [Nm] [1], 0.25 [Nm] [2]
	4th joint	0.04 [Nm] [1], 0.02 [Nm] [2]
Gear ratio of the thumb	1st joint	713.43:1
	2nd joint	384.69:1
	3rd joint	148.48:1
	4th joint	80.00:1
Band width of the thumb	1st joint	10.4 [Hz]
	2nd joint	12.3 [Hz]
	3rd joint	7.4 [Hz]
	4th joint	9.5 [Hz]

[1]Maximum output,   [2]Rated output
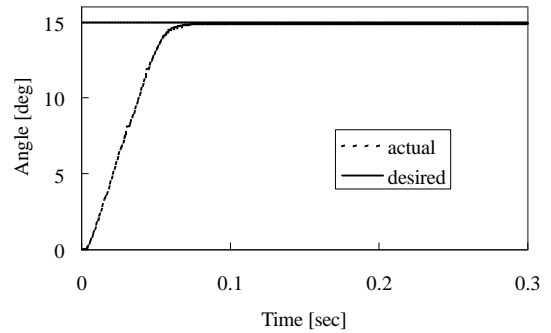
Fig. 4. Step responses of the 1st joint of the thumb

transmission, dummy gears which are allocated symmetrically to the axis of the first joint are introduced. Moreover, a set collar is introduced to prevent the face gear from relaxing. By these modifications, the backlash of the second joint of the thumb is decreased to less than 1.0 degree. The backlash of the other joints also decreased by nearly the same amount.

2.2.2 Higher Response
A step response of the first joint of the thumb by PD control is shown in Fig. 4. The bandwidth of the frequency characteristics at velocity feedback is 10.4 Hz. The other joints were also measured similarly, and the results are shown in Table 1. The minimum bandwidth of the robot hand is 7.4 Hz, which is approximate to that of Gifu Hand II. The bandwidth of the human finger is, at most, 5.5 Hz. This means that the robot hand can move more quickly than the human hand.

2.2.3 Opposability of the Thumb
The thumb of the human hand can move in opposition to the fingers. Dexterity of the human hand in object manipulation is
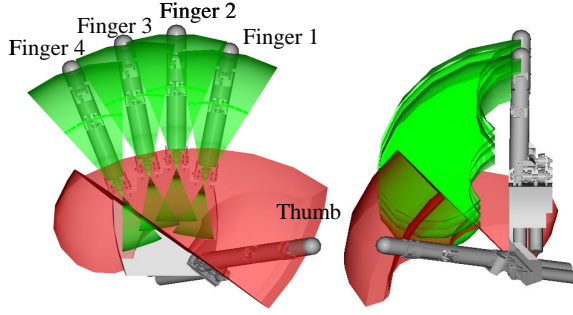
joints with 16 DOF. Each servomotor has a magnetic encoder with 16 pulses per revolution. Table 1 summarizes the characteristics of the Gifu hand III.

2.2 Improvements Over Gifu Hand II
The mechanism of Gifu Hand III is improved over that of Gifu Hand II [16] as described in the following.

2.2.1 Reduction of Backlash in the Transmission
In the Gifu Hand II, the maximum backlash was almost 1.0 degree. However, the backlash increased to more than 5.0 degrees after a long operation. To reduce the backlash caused by the tilt of the face gear and advance the efficiency of the

Fig. 5. Mobility space

Table 2. Opposability of the thumb

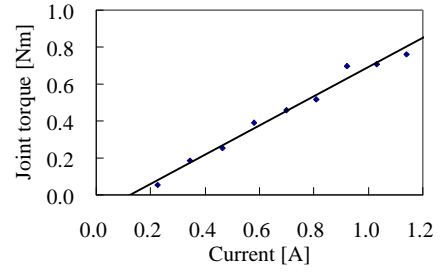|	
v_1 [cm³]	6.25 x 10
v_2 [cm³]	4.75 x 10
v_3 [cm³]	4.99 x 10
v_4 [cm³]	1.29 x 10
J	4.49 x 10⁻²

Fig. 6. Relation between the current and torque

(a) Skeleton

(b) Relation between the third and fourth joints angles

Fig. 7. Planar four-bars linkage mechanism

caused by the thumb opposability. The robot hand was designed as such it has high opposability of the thumb.

The operating angles of joints are shown in Table 1. The operating area of the robot hand is larger than that of Gifu Hand II. Therefore, the allocation of the fingers was modified to enhance the opposability of the thumb as shown in Fig. 3. Fig. 5 shows the mobility space of fingertips for Gifu Hand III. A performance index of the thumb opposability is defined by

$$J = \frac{1}{d^3} \sum_{i=1}^{k} w_i \, v_i \,, \qquad (1)$$

where v_i denotes the volume of intersection between the mobility space of the thumb and that of the i-th finger, k denotes the number of the finger except the thumb, d is the length of the thumb, and w_i is a weighting coefficient. Table 2 shows v_i for the case of Gifu Hand III. J of the robot hand is 4.49x10⁻², while that of the Gifu Hand II is 1.20x10⁻². In either case, all weighting coefficients are equal to 1.00. Therefore, the performance index of Gifu Hand III is 3.75 times better than that of Gifu Hand II.

2.2.4 16ch Power Amplifier

The 16ch power amplifier of the Gifu Hand III has a monitoring function of electric currents. It is found that electric current changes in proportion to the motor load. Fig. 6 shows the relationship between the joint torque t and the electric current I for the second joint of the thumb. From Fig. 6, an approximate expression is deduced

$$t = 0.79 \, I - 0.098 \,. \qquad (2)$$

Therefore, the static friction torque of the joint is about 0.098 Nm. The other joints torques change similarly in proportion to the electric currents.

2.3 Planar Four-Bars Linkage Mechanism

In the human hand, the fourth joint angle engages with the third joint angle almost linearly [14]. In the Gifu Hand III, the fourth joint is driven by a planar four-bars linkage mechanism shown in Fig. 7 (a). The relation between the third joint angle
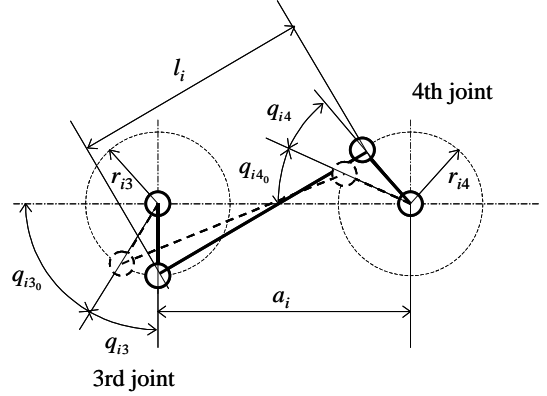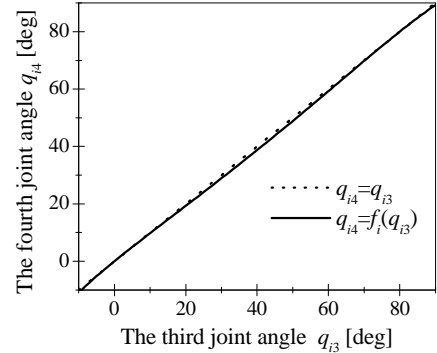
and the fourth joint angle is given as follows:

$$l_i = \left[\left\{ r_{i3} \sin(q_{i3_0} + q_{i3}) + r_{i4} \sin(q_{i4_0} + q_{i4}) \right\}^2 \right. \\ \left. + \left\{ a_i + r_{i3} \cos(q_{i3_0} + q_{i3}) - r_{i4} \cos(q_{i4_0} + q_{i4}) \right\}^2 \right]^{\frac{1}{2}} \,, \qquad (3)$$

where a_i is the length of the finger second segment, r_{i3} and r_{i4} are the link radiuses of the third and fourth joints, q_{i3_0} and q_{i4_0} are the initial angles of the planar four-bars linkage mechanism, l_i is the length of the connection link, and the suffix i refers to the i-th finger. Eq. (3) is satisfied for an arbitrary q_{i3_0} and q_{i4_0}, because l_i is a constant value. The previous paper [14] proposed a recursive numerical computation method of the fourth joint angle. This approach is time consuming. By detail analysis, an explicit relation

between the third joint angle and the fourth joint angle is derived as follows:

$$q_{i4} = f_i(a_i, r_{i3}, r_{i4}, q_{i3_0}, q_{i4_0}, q_{i3})$$
$$= \sin^{-1}\left(\frac{c_{i1}}{\sqrt{c_{i2}^2 + c_{i3}^2}}\right) - \tan^{-1}\left(\frac{c_{i2}}{c_{i3}}\right) - q_{i4_0} \quad (4)$$

where

$$c_{i1}(a_i, r_{i3}, r_{i4}, q_{i3_0}, q_{i4_0}, q_{i3})$$
$$= -2\,r_{i3}\,r_{i4}\cos\!\left(q_{i3_0}+q_{i4_0}\right)$$
$$+2\,a_i\,r_{i3}\cos q_{i3_0} - 2\,a_i\,r_{i4}\cos q_{i4_0} ,$$
$$-2\,a_i\,r_{i3}\cos\!\left(q_{i3_0}+q_{i3}\right)$$
$$c_{i2}(a_i, r_{i3}, r_{i4}, q_{i3_0}, q_{i3})$$
$$= -2\,a_i\,r_{i4} - 2\,r_{i3}\,r_{i4}\cos\!\left(q_{i3_0}+q_{i3}\right),$$
$$c_{i3}(r_{i3}, r_{i4}, q_{i3_0}, q_{i3}) = 2\,r_{i3}\,r_{i4}\sin\!\left(q_{i3_0}+q_{i3}\right). \quad (5)$$

The explicit equation contributes to reduce the computation time of q_{i4}. In the case of Gifu Hand III, the parameters are set as follows: $a_i = 32$ mm, $r_{i3} = r_{i4} = 7$ mm, $q_{i3_0} = 70$ deg, $q_{i4_0} = 30$ deg. As a result, the relation between q_{i3} and q_{i4} is shown in Fig. 7 (b). The line and the dotted line denote the actual fourth joint angle and the linear approximation, respectively. A maximal difference from the linear approximation is 1.27 deg at $q_{i3} = 40.6$ deg. This shows that the fourth joint of the robot finger can engage with the third joint almost linearly like a human finger.

3. Distributed Tactile Sensor

A developed distributed tactile sensor in cooperation with Nitta Corporation for the Gifu Hand III is shown in Fig. 8. The tactile sensor is mounted on the surface of the fingers and palm. The tactile sensor has grid pattern electrodes and uses conductive ink in which the electric resistance changes in proportion to the pressure on the top and bottom of a thin film. The characteristics of the tactile sensor are shown in Table 3. The numbers of detecting points on the palm, the thumb, and each of the fingers are 313, 126, and 105, respectively, and the total number of detecting points is 859. As a result, the tactile sensor for Gifu Hand III presents 235 points expansion relatively to that of Gifu Hand II. The electrode column width is 3.0 mm, the electrode row width is 3.7 mm, the column pitch is 4.0 mm, and the row pitch is 4.7 mm. Therefore, the insensitive area, which means an ummeasurable area even if the contact happens, of the tactile sensor is reduced to 49.1 %. The maximum load is about 2.2×10^{-3} N/m^2, the resolution of measurement is 8 bits, and the sampling cycle is 10 ms/frame. The response characteristic of the tactile sensor is more than 1 kHz. The detected data on the sensor sheet is transported to a PC through a special interface board.

4. Experiments

To realize the skill of human grasping for the robot hand, experiments using a grasping strategy [17], which imitates the grasping reflex of a baby of about 10 months of age, are shown.
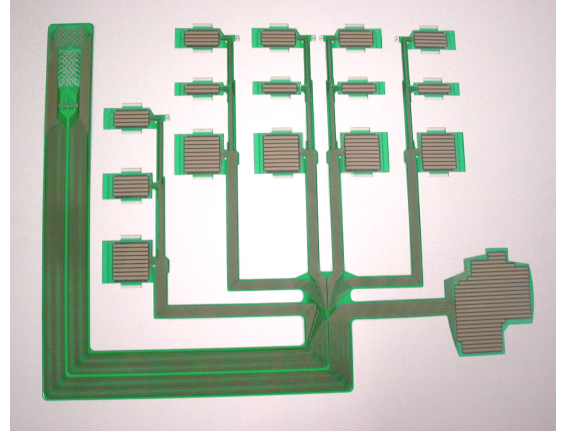

Fig. 8. Developed distributed tactile sensor

Table 3. Characteristics of the tactile sensor

Number of detecting points	
Total	859
Palm	313
Thumb	126
Finger	105
Maximum load	2.2×10^{-3} [N/m^2]
Electrode column width	3.0 [mm]
Electrode row width	3.7 [mm]
Column pitch	4.0 [mm]
Row pitch	4.7 [mm]
Sampling cycle	10 [ms/flame]
Resolution	8 [bit]
Thickness of sensor sheet	0.2 [mm]
Weight	18 [gf]

4.1 Grasping Strategy Imitating Human Grasping Reflex

A Grasping strategy imitating grasping reflex is presented and is very simple. The strategy is summarized in the following. Fig. 9 shows a contact state between an i-th finger and an object, where q_{ij} and F_{ij} are respectively the angle of the j-th joint and the total contact force of the j-th link, of the i-th finger. The grasping reflex includes two stages: grasping action, which occurs at the object contact with the hand, and keeping action, which occurs at the object removal form the hand. In a grasping action, each finger contacts the object with a uniform force. This approach will enhance the possibility of grasping unknown objects because the number of contact points is maximized and the thumb and the fingers envelop the object. When the object contacts the hand, joints 2 to 4 of the thumb and the fingers are controlled independently to generate flexion such that the force of adjacent fingertip side link of each joint equals a desired force. A velocity control and a force control are adopted at non-contact state and contact state, respectively. The motor input E_{ij}, which drives the j-th joint of the i-th finger, is given by

$$E_{ij} = -K_{Vij}\left(\dot{q}_{ij} - \dot{q}_{dij}\right) \quad (i=1,\cdots,5; j=2,\cdots,4), \quad (6)$$

where K_{Vij} is the velocity feedback gain of the j-th joint of the i-th finger, and $\dot{q}_{dij}$ is the desired velocity of the j-th joint
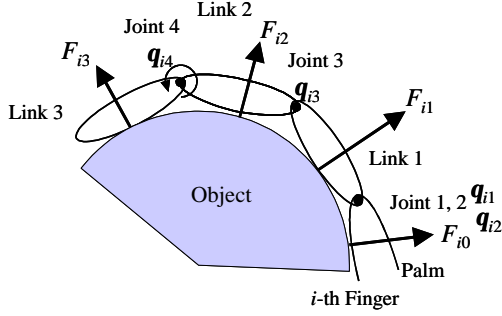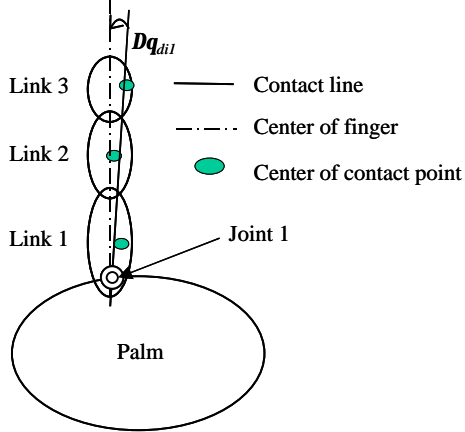
Fig. 9. Links and contact forces

Fig. 10. Desired joint angle of the first joint
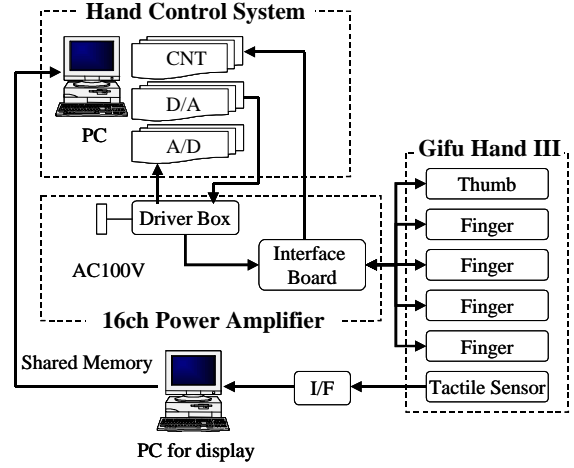

Hand Control System

Fig. 11. Experimental system

(a) Sphere   (b) Cylinder

(c) Prism

Fig. 12. Grasping various objects

of the i-th finger. The desired velocity of each joint is given by

$$\dot{\boldsymbol{q}}_{d\,ij} = \begin{cases} \dot{\boldsymbol{q}}_{c\,ij} : \text{non - contact state} \\ -K_{f\,ij}\left(F_{ij} - F_{d\,ij}\right) - K_{fl\,ij}\int\left(F_{ij} - F_{d\,ij}\right)dt, \\ \qquad\qquad\qquad\qquad\qquad : \text{contact state} \end{cases} \quad (7)$$

where $K_{f\,ij}$ is the force feedback gain, and $K_{fl\,ij}$ is the force integral gain. The link at contact sate is controlled by force feedback control. The fourth joint of each of the fingers, excluding the thumb, of Gifu Hand III cannot be driven directly as mentioned above. Hence, if only either the third link or the fourth link is in contact with the object, then the desired force of the third joint is obtained by adopting the largest of F_{i3} and F_{i4}.

The first joint is controlled to generate abduction and adduction according to the object size. The first joint of each of the thumb and the fingers is controlled by position and velocity control given by

$$E_{i1} = -K_{p\,i1}\left(\boldsymbol{q}_{i1} - \boldsymbol{q}_{d\,i1}\right) - K_{V\,i1}\dot{\boldsymbol{q}}_{i1} \quad (i = 1,\cdots,5), \quad (8)$$

where $K_{p\,i1}$ is the position feedback gain, and $\boldsymbol{q}_{d\,i1}$ is the desired joint angle. The desired joint angle is designed as such a center line on the surface of each of the thumb and the fingers coincides with a contact line, which is lined from the axis of the first joint to the contact points using the least square method as shown in Fig. 10.

4.2 Experimental System
Fig. 11 shows a developed PC-based control system for the experiments. Counter boards, D/A boards, and A/D boards are
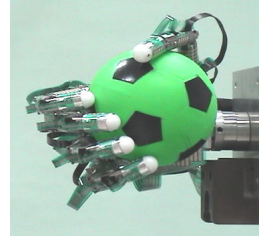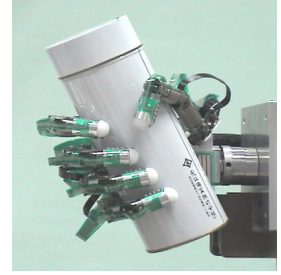
connected to the PCI bus of a PC. The maximum output of the D/A board is ±5 V. The signals of the D/A board are inputted to servomotors through a 16ch power amplifier with 3.6 gain. The operating system of the PC is either ART-Linux, which is a real-time operating system, or Windows 98. The tactile sensor output is processed by a PC with a 10 ms period. The measured tactile data is transported to a hand control PC through a shared memory (named Memolink, Interface Co.). The sampling cycle of the hand controller is 2 ms.

4.3 Experimental Results
Fig. 12 shows the grasping of various objects, which are a sphere with a diameter of 11.0 cm, a cylinder with a diameter of 8.0 cm, and a quadratic prism of 6.5 cm x 7.5 cm on the top and bottom. The desired contact force is of 0.3 N. In the case of the sphere, the contact force responses are shown in Fig. 13. They show that the contact force of each link is close to the desired force. It happens that either link 2 or link 3 of a finger does not contact the object because the fourth joint is engaged
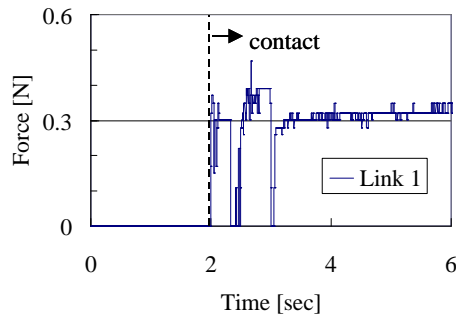
(a) Link 1
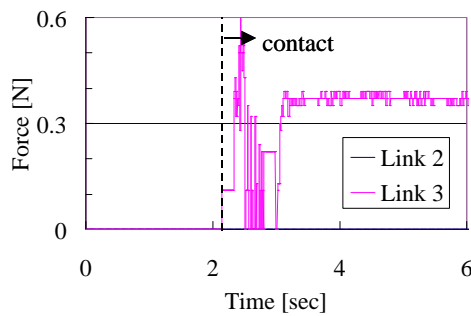
(b) Link 2 and 3

Fig. 13. Contact force

with the third joint. In human fingers, the fourth joint curves at strong grasping and makes the grasping more stable.

5. Conclusions

Newly developed anthropomorphic robot hand named Gifu hand III has been presented. The robot hand is actuated by built-in servomotors and can be equipped with a 6-axes force sensor at each fingertip. A distributed tactile sensor with 859 detecting points can be attached to the surface of the fingers and palm. The backlash of transmission, the mobility space, and the opposability of the thumb are improved relatively to Gifu Hand II. The response of the Gifu Hand III fingers exceeds that of the human fingers and consequently the robot hand can move more quickly than the human hand. Experiments of grasping several objects have been shown. The control system for the Gifu Hand III runs on ART-Linux, which is a real-time operating system. The Gifu Hand III is planned to be used for future studies on dexterous grasping and manipulation by a robot.

Acknowledgements

References

[1] J. K. Salisbury and J. J. Craig, "Articulated Hands: Force Control and Kinematic Issues", *Int. J. Robot. Res.*, Vol. 1, No. 1, pp. 4-17, 1982.

[2] S. C. Jacobsen, J. E. Wood, D. F. Knutti, and K. B. Biggers, "The Utah/MIT dexterous hand: Work in progress", *Int. J. of Robot. Res.*, Vol. 3, No. 4, pp. 21-50, 1984.

[3] B. M. Jau, "Dexterous Telemanipulation with Four Fingered Hand System", *Proc. of IEEE Robo. and Automa.*, pp. 338-343, 1995.

[4] K. J. Kyriakopoulos, A. Zink, and H. E. Stephanou, "Kinematic Analysis and Position/Force Control of the Anthrobot Dextrous Hand", *Trans. on System, Man, and Cybernetics-Part B: cybernetics*, Vol. 27, No. 1, pp. 95-104, 1997.

[5] G. A. Bekey, R. Tomovic and I. Zeljkovic, "Control Archtecture for the Bergrade/USC hand", In S. T. Venkataraman and T. Iberall(Editors), Dexterous Robot Hand, Springer Verlay, pp.136-149, 1990.

[6] M. Rosheim, "Robot Evolution", John Wiley & Sons, Inc., pp.216-224, 1994.

[7] L. R. Lin and H. P. Huang, "Integrating Fuzzy Control of the Dexterous National Taiwan University (NTU) Hand", *IEEE/ASME Trans. on Mechatronics*, Vol. 1, No. 3, pp. 216-229, 1996.

[8] J. Butterfass, M. Grebenstein, H. Liu, G. Hirzinger, "DLR-Hand II: Next Generation of a Dextrous Robot Hand", *Proc. of IEEE Int. Conf. on Robo. and Automa.*, pp. 109-114, 2001.

[9] R. S. Fearing, "Tactile Sensing Mechanisms", *Int. J. of Robot. Res.*, Vol. 9, No. 3, pp. 3-23, 1990.

[10] R. D. Howe, "Tactile Sensing and control of robotic manipulation", *Advanced Robotics*, Vol. 8, No. 3, pp. 245-261, 1994.

[11] M. Shimojo, S. Sato, Y. Seki, and A. Takahashi, "A System for Simulating Measuring Grasping Posture and Pressure Distribution", *Proc. of IEEE Int. Conf. on Robo. and Automa.*, pp. 831-836, 1995.

[12] D. Johnston, P. Zhang, J. Hollerbach, and S. Jacobsen, "A Full Tactile Sensing Suite for Dextrous Robot Hands and Use In Contact Force Control", *Proc. of IEEE Int. Conf. on Robo. and Automa.*, pp. 3222-3227, 1996.

[13] J. Jockusch, J. Walter, and H. Ritter, "A Tactile Sensor System for a Three-Fingered Robot Manipulator", *Proc. of IEEE Int. Conf. on Robo. and Automa.*, pp. 3080-3086, 1997.

[14] H. Kawasaki and T. Komatsu, "Development of an Anthropomorphic Robot Hand Driven by Built-in Servo-motors", *Proc. of the 3rd Int. Conf. On ICAM*, Vol. 1, pp. 215-220, 1998.

[15] H. Kawasaki and T. Komatsu, "Mechanism Design of Anthropomorphic Robot Hand: Gifu Hand I", *J. of Robot. and Mechatronics*, Vol. 11, No.4, pp. 269-273, 1999.

[16] H. Kawasaki, Tsuneo Komatsu, Kazunao Uchiyama, and Takashi Kurimoto, "Dexterous Anthropomorphic Robot Hand with Distributed tactile Sensor: Gifu Hand II", *Proc of 1999 IEEE ICSMC*, Vol. II, pp. II782-II787, 1999.

[17] H Kawasaki, T. Mouri, J. Takai, and S. Ito, "Grasping of Unknown Object Imitating Human Grasping Reflex", *CD-ROM of preprints of the 15th IFAC World Congress*, 2002.